Based on transcriptome and metabolome analyses, a preliminary study on the causes of changes in paintings during Hibiscus syriacus flowering

Zhezhe LI
Hebei Normal University of Science and Technology
Dan LIU
Shandong Provincial Forest and Grass Germplasm Resources Center
Dongsheng WANG
Hebei Normal University of Science and Technology
Meng SUN
Hebei Normal University of Science and Technology
Guojun ZHANG
Hebei Normal University of Science and Technology
Yu WU
Hebei Normal University of Science and Technology
Yidan ZHANG
Hebei Normal University of Science and Technology
Bei-bei Cheng (beibei87613@126.com)
Hebei Normal University of Science and Technology

Research Article

Keywords: Hibiscus syriacus, Transcriptome sequencing, Flower color change, Flavonoid

Posted Date: August 29th, 2023

DOI: https://doi.org/10.21203/rs.3.rs-3240925/v1

Abstract

Background

The flower color of *H. syriacus* 'Qiansiban' undergoes a transition from fuchsia to pink purple and finally to pale purple, thereby enhancing the ornamental value of the cultivars. However, the molecular mechanism underlying flower color change is still unclear in *H. syriacus*. In this study, the transcriptomic data of *H. syriacus* 'Qiansiban' at five developmental stages were analyzed to investigate the impact of flavonoid components on flower color variation. Additionally, five cDNA libraries were constructed from *H. syriacus* 'Qiansiban' during critical blooming stages, and the transcriptome was sequenced to investigate the molecular mechanisms underlying changes in flower coloration.

Results

High-performance liquid chromatography—mass spectrometry detected five anthocyanins in *H. syriacus* 'Qiansiban', with malvaccin-3-*O*-glucoside being the predominant compound in the flowers of *H. syriacus* at different stages, followed by petunigenin-3-*O*-glucoside. The levels of these five anthocyanins exhibit a gradual decline throughout the flowering process. In terms of the composition and profile of flavonoids and flavonols, a total of seven flavonoids were identified: quercetin-3-glucoside, luteolin-7-*O*-glucoside, Santianol-7-*O*-glucoside, kaempferol-*O*-hexosyl-C-hexarbonoside, apigenin-C-diglucoside, luteolin-3,7-diglucoside, and apigenin-7-*O*-rutinoside. A total of 2702 differentially expressed genes were identified based on the selected reference genome. Based on the enrichment analysis of differentially expressed genes, we identified 9 structural genes (PAL, CHS, FLS, DRF, ANS, CHI, F3H, F3'5'H, and UFGT) and 7 transcription factors (3 MYB, 4 bHLH) associated with flavonoid biosynthesis. The qRT—PCR results were in good agreement with the high-throughput sequencing data.

Conclusion

This study will establish a fundamental basis for elucidating the mechanisms underlying alterations in the flower pigmentation of *H. syriacus*.

Introduction

Hibiscus syriacus L., a perennial deciduous shrub or small tree, belongs to the family Malvaceae and genus *Hibiscus*. Its cultivars are rich in color, including red, pink, purple, blue, and white. The trees are full flowers in full bloom and have high ornamental value. The flowering period of individual *H. syriacus* is short and lasts only one day, so it is also known as blooming in the morning and falling in the evening. Although the flowers have a short lifespan, some cultivars change flower color during the flowering process, such as 'Qiansiban'. Its flower colorchanges from fuchsia to pink purple then to pale purple. This characteristic confers high ornamental and research value to this cultivar. In fact, many plants change flower color during flowering. Paeonia 'Coral Sunset' and 'Pink Hawaiian Coral' flowers change from coral to pink then to pale yellow during flowering [1]. The corolla of purple—red *M. jalapa* changed from light green to purple—red between budding and blooming [2].

Flower color, an important ornamental trait of plants, can be affected by anthocyanin, cell sap pH, and metal ions. Among these, the anthocyanin component and content are the most important factors. There are three main types of pigments related to flower color formation: flavonoids [3], carotenoids [4], and alkaloids [5]. Flavonoids mainly include anthocyanins, flavones, and flavonols [6]. At present, 27 categories of anthocyanins have identified in nature, of which only 6 are the most common, namely, cyanidin, geranium, delphinidin, paeoniflorin, Petunia, and Mallow [5]. Geranium is usually orange to red, cyanidin is pink, delphinidin is blue to purple, and flavonoids and flavonols are colorless or

light yellow, which generally affects the formation of flower color as copigments [7]. Zhang et al. [8] detected major anthocyanins of *H. syriacus*, including cyanidin, geranium, delphinidin, paeoniflorin, and Petunia. In addition, the flavonoid biosynthetic pathway was studied in detail. In the flavonoid metabolic pathway, the expression of genes such as CHS, CHI, and DRF promotes the synthesis of anthocyanins and contributes to the color coloration of *H. syriacus* [9].

However, the mechanism underlying color change in *H. syriacus* during flowering is still unclear. To investigate the mechanism, *H. syriacus* 'Qiansiban', which change flower color during flowering, were selected as experimental materials. In this study, flavonoids of petals at five developmental stages was identified by high-performance liquid chromatography–mass spectrometry (HPLC–MS) and the relationship between flower coloration and pigment content was analyzed. Furthermore, a comparative transcriptomic analysis of five critical states of flowering in 'Qiansiban' was conducted to identify the differentially expressed genes (DEGs) related to flavonoid biosynthesis. This research would be helpful to elucidate the mechanism of flower color change in *H. syriacus*.

Material and methods

Plant Materials

Petals of 'Qiansiban' were used as experimental materials. Samples were collected at five different flowering stages (S1, S2, S3, S4, S4, S5) in July 2021 at Hebei Normal University of Science and Technology. Materials for tests were placed in liquid nitrogen immediately and stored at − 80°C.

Anthocyanin quantification

Flower petals were collected at five sequential developmental stages: splitting stage (S1), early stage (S2), initial opening period (S3), blooming period (S4), and final flowering stage (S5). Taking 0.1 g of the corolla partfrom different periods, grind them into powder with liquid nitrogen, respectively, transfer them to a 10 mL centrifuge tube, add 5 mL1% hydrochloric acid methanol solution, shake them well, and then fully soak them in a 4 ℃ refrigerator under dark conditions for 24 h (multiple shocks during this period), centrifuge them for 15 min (4℃, 13000r·min^{-1}), and take the supernatant. Finally, the content of anthocyanins was determined by HPLC–MS.

Wherein: liquid phase condition: column temperature 40 ℃, injection volume 10.0 μL. The flow rate was 0.50 mL/min, and the absorption spectra were scanned at wavelengths of 350 nm and 520 nm. Mobile phase parameters: A was a formic acid aqueous solution with a volume fraction of 1%, and B was chromatographic acetonitrile. The gradient elution procedure was as follows: 0 min, 95% A + 5% B; 40 min, 60% A + 40% B; 45 min, 95% A + 5% B. The analysis time was 80 min.

Mass spectrum conditions: positive ion mode, electric spray ion source, dryer temperature 400 ℃, ion source temperature 120 ℃, drying airflow speed 10 L/min, spray gas pressure 50 psi, capillary cracking voltage 3.5 kV, cone hole voltage 40 V, mass scanning range: m/z 100–1200.

With standard cyanidin and rutin as the control, concentration as the abscissa, and peak area as the ordinate, the standard curve was made to calculate the content of anthocyanins and flavonoids.

The standard equation of cyanidin content is y = 528.57x-9.6762 R2 = 0.9989; the standard equation of rutin content is y = 534.58x + 499.02 R2 = 0.996.

RNA extraction, cDNA library construction, and transcriptome sequencing

Total RNA was extracted using the RNA prep Pure Plant Kit (Tiangen, Beijing, China) according to the instructions provided by the manufacturer. A total amount of 1 μg RNA per sample was used as input material for the RNA sample preparations. Sequencing libraries were generated using the Hieff NGS Ultima Dual-mode mRNA Library Prep Kit for Illumina (Yeasen Biotechnology (Shanghai) Co., Ltd.) following the manufacturer's recommendations, and index codes were added to attribute sequences of each sample. First strand cDNA was synthesized, and second strand cDNA synthesis was subsequently performed. The remaining overhangs were converted into blunt ends via exonuclease/polymerase activities. After adenylation of the 3' ends of DNA fragments, NEBNext Adaptor with hairpin loop structure was ligated to prepare for hybridization. The library fragments were purified with the AMPure XP system (Beckman Coulter, Beverly, USA). Then, 3 μl USER Enzyme (NEB, USA) was used with size-selected, adaptor-ligated cDNA at 37°C for 15 min followed by 5 min at 95°C before PCR. Then, PCR was performed with Phusion High-Fidelity DNA polymerase, Universal PCR primers, and Index (X) Primer. Finally, PCR products were purified (AMPure XP system), and library quality was assessed on the Agilent Bioanalyzer 2100 system. The libraries were sequenced on an Illumina NovaSeq platform to generate 150 bp paired-end reads, according to the manufacturer's instructions.

De novo assembly and annotation

Raw reads were filtered by removing adaptor sequences and low-quality sequences to obtain high-quality reads. Gene function was annotated based on the following databases: Nr (NCBI nonredundant protein sequences); Pfam (Protein family); KOG/COG (Clusters of Orthologous Groups of proteins); Swiss-Prot (a manually annotated and reviewed protein sequence database); KO (KEGG Ortholog database); and GO (Gene Ontology).

Verification by qRT—PCR analysis

The expression of key genes in the petals of 'Qiansiban' was measured using RT—qPCR. A 10 μl reaction system was formulated based on the instructions of TB Green TaKaRa Premix Ex Taq™ II (Tli RNaseH Plus; TaKaRa Bio Inc., Japan). Amplification proceeded as follows: predenaturation at 95°C for 30 s, 40 cycles at 95°C for 5 s, annealing for 30 s and 60°C for 30 s. Dissolution curves were recorded from 65°C to 95°C with a 0.5°C increase every 5 s. Each reaction was repeated three times. The relative expression level of target genes was calculated by $2^{-\Delta\Delta Cq}$, and relevant data were analyzed by SPSS version 26.

Results

Qualitative and quantitative analysis of anthocyanins

Table 1
Chromatographic and spectral data of anthocyanina from 'Qiansiban'.

Peak	Retention time (min)	Molecularion	Fragmention	Tentative identification
1	11.4	465.1	303.05	Delphinidin-3-*O*-glucoside
2	13.2	449.1	287.05	Cyanidin-3-*O*-glucoside
3	13.95	479.11	317.06	Petunidin-3-*O*-glucoside
4	14.84	433.11	271.06	Pelargonidin-3-*O*-glucoside
5	16.3	493.13	331.08	Malvacin-3-*O*-glucoside
6	11.28	465.1	303.05	Quercetin-3-glucoside
7	13.07	449.1	287.05	Luteolin-7-*O*-glucoside
8	14.14	451.12	289.07 199.01	Santianol-7-*O*-glucoside
9	16.28	611.15	499.1	Kaempferol-O-hexose-C-hexoside
10	16.66	595.16	433.11 313.07	Apigenin-C-diglucoside
11	17.13	611.15	499.1	Luteolin-3,7-diglucoside
12	19.9	579.16	433.11	Apigenin-7-*O*-rutoside

The color of flower samples varies from S1 to S5. (B): Total contents of individual anthocyanidins at S1 to S5. The bars represent the average data of the three operations of HPLC–MS/MS.

Flower color of 'Qiansiban' is purplish red at S1 stage, and as the flowers bloom, the color gradually changes to pinkish purple and to purple finally (Fig. 1A).

Anthocyanins and flavones/flavonols were identified by comparison with the HPLC retention time, elution order, UV–vis spectrum and MS fragmentation pattern in published data (Table 1).

Through the analysis of mass spectrometry molecular ions and fragment ions and in combination with references [10, 11, 12], five anthocyanins were detected in the petal of 'Qiansiban' at five stages, namely, delphinidin-3-*O*-glucoside (De3G), cyanidin-3-*O*-glucoside (Cy3G), petunidin-3-*O*-glucoside (Pe3G), pelargonidin-3-*O*-glucoside (Pg3G), and malvacin-3-*O*-glucoside (Ma3G) (Table 1). It is speculated that the 7 flavonoes and flavonols were quercetin-3-glucoside, luteolin-7-*O*-glucoside, santianol-7-*O*-glucoside, kaempferol-O-hexose-C-hexoside, apigenin-C-glucoside, luteolin-3,7-diglucoside, and apigenin-7-*O*-rutoside (Table 1) [13, 14, 15].

H. syriacus petals undergo major changes in flavonoid and anthocyanin accumulation from S1 to S5. Anthocyanidin is the main contributor to the color of *H. syriacus*, thus the type, content, and biosynthesis process of flavonoids in *H. syriacus* petals are analyzed emphatically.

The highest flavonoid content was found at S1, which gradually decreased with the flower opening process. The higher content of anthocyanidin in S1 was Ma3G (Fig. 1B), and the higher content of flavonoe and flavonol were apigenin-C-diglucoside (Supplementary Table S1). The accumulation trend of flavonoes and flavonols were S1 > S2 > S3 > S4 > S5, showing a gradually decreasing trend. The analysis based on HPLC–MS/MS shows that all anthocyanidins have the highest content in S1 and the lowest content in S5. The contents of these five anthocyanins

gradually decreased with the flowering process; from S1 to S5, they decreased by 46%, 52%, 40%, 64%, and 39%, respectively.

In summary, the accumulation of flavonoids and anthocyanidin reached highest and lowest at S1 and S5 respectively. Ma3G (anthocyanidin content with high accumulation content), De3G, Pe3G, Cy3G, and Pg3G are the main chromogenic anthocyanidins. With the decrease in anthocyanidin concentration, the color of the petals changed from purplish red to purple (Fig. 1).

Transcriptome profiling of H. syriacus petals in different states

Overview of transcriptome sequencing

Transcriptome sequencing was performed on 15 samples at 5 stages of 'Qiansiban'. A total of 89 Gb clean data was obtained, and the clean data of each sample reached 6.616 Gb. The GC content was 44.34% − 45.62%, and the percentage of the Q30 base was 93.62% − 95.03% (Supplementary Table S2).

Functional annotation of new genes

The DIAMOND [16] code was used to match the newly discovered sequence with the NR [17], Swiss professional [18], COG [19], KOG [20], and KEGG [21] databases, and the KEGG origin and alternative results of the new sequence were obtained. InterProScan [22] used the info integrated by InterPro to investigate the GO [23] GO Orthology results of the latest genes, foreseen the aminoalkanoic acid sequence of the latest genes, and then compared them with the Pfam [25] database victimization HMMER [24] code to obtain annotation data of the latest genes.

Based on the chosen order, the mapped reads were spliced with the NeighborTie code, and compared with the first-order annotation data, 32956 new genes were discovered, of which 23322 were annotated. The genes annotated in different databases range from 4319 to 23235, with TrEMBL annotation having the highest number of genes and COG annotation having the lowest number of genes (Table 2).

Table 2
Statistics of annotation results of new gene functions

Annotated databases	COG	GO	KEGG	KOG	Pfam	Swiss-Prot	TrEMBL	eggNOG	NR	All
New Gene Number	4,319	15,725	13,795	11,717	12,552	14,343	23,235	18,006	23,052	23,322

Analysis of DEGs identified in the four libraries

With thresholds FDR < 0.01 and FC > 2, 3456 DEGs (3 053 up- and 403 downregulated) were found between the FS1 and FS2 libraries. Meanwhile, the number of differential expressed genes between the FS1 and FS3 libraries is the most, with 27 736 DEGs (12 655 up- and 15 081 downregulated) found. 25 968 DEGs (12 124 up- and 13 844 downregulated) were found between the FS1 and FS4 libraries, and 20 937 DEGs (10 013 up- and 10 924 downregulated) between the FS1 and FS5 libraries were detected (Fig. 2A). The common differential expressed genes among 5 comparisons were 2702 (Fig. 2B).

GO enrichment analysis was conducted on the screened differentially expressed genes, and Fig. 3A shows the top 20 classifications with the highest GO enrichment of differentially expressed genes. The differentially expressed genes are distributed in the three primary classifications of biological process, cell composition, and molecular operation.

Mainly enriched in cell process, biological process, and single-organism process in biological process, catalytic activity, binding, and transporter activity in cell composition, and cell, cell part, and organelle in molecular operation.

The differential factor KEGG metabolic pathway map is especially integrated into a whole metabolic pathway by classifying the differential genes. KEGG metabolic pathway of the ‘Qiansiban’ differential factor primarily focuses on essential amino acid synthesis, flavonoid synthesis, cyanide metabolism, flavonoid and flavonol synthesis, essential amino acid metabolism, and anthocyanin synthesis. Among them, the metabolic pathways associated with flower color formation are essential amino acid synthesis and metabolism, flavonoid and flavonol synthesis, and anthocyanin synthesis (Fig. 3B).

By analyzing the sequences of the transcriptome of *H. syriacus*, combined with KEGG annotation, sixty-four differentially expressed genes were obtained at the 5 stages of 'Qiansiban'. The utmost variety of UFGT genes was fourteen, and the minimum variety of F3'5'H genes was one (Fig. 3C).

Identification of structural genes of interest in the flavonoid synthesis pathway

Transcriptome analysis showed that sixty-four genes were considerably enriched in the flavonoid biogenesis pathway. The accumulation patterns of these anthocyanidins at different stages were consistent. The relative expression level of PAL sequentially decreases when reaching its most worth at S2 and increased at S5. The relative expression levels of CHS1 and ANS1 genes additionally reached their most throughout the S2 amount, with the CHS1 sequence step by step decreasing throughout the S2-S5 amount and the ANS1 sequence increasing throughout the S4 amount and decreasing throughout the S5 amount. The relative expression level of the CHI1 sequence step by step decreased throughout the S1-S4 amount and increased throughout the S5 amount. The relative expression level of the FLS1 sequence is strictly the other, step by step increasing throughout the S1-S4 amount and decreasing throughout the S5 amount. The relative expression level of the DFR1 sequence step by step decreased throughout the S1-S5 amount. Among the relative expression levels of the UFGT1 sequence, the relative expression level was the lowest within the S2 stage and increased from the S2-S5 stage. The relative expression levels of F3H3 associated with nursingd F3'5'H genes showed an increasing decreasing trend, reaching their most values throughout the S4 and S2 periods (Figs. 4 and 5, Supplementary Table S3 and Table S6).

According to the GO enrichment map and KEGG enrichment map of DEGS, nine structural genes were screened, which played a key role in the flower color change of 'Qiansiban', namely, UFGT1(gene-LOC120143098), DFR1(gene-LOC120216676), CHI1(gene-LOC120193176), FLS1(gene-LOC120188023), ANS1(gene-LOC120214326), CHS1(Hibiscus_syriacus_newGene_21723), PAL1(Hibiscus_syriacus_newGene_32513), F3'5'H(Hibiscus_syriacus_newGene_29100) and F3H(gene-LOC120154124).

Changes in the expression of transcription factors

Transcription factors such as MBW (MYB, bHLH, WD40) affect the color of *H. syriacus* flowers by regulating the synthesis of anthocyanins. According to transcriptome sequencing and classification statistics, the number of five transcription factors, including AP2-ERF-EFR, MYB, bHLH, C2H2, and NAC (Supplementary Figure S1), are relatively high in the 'Qiansiban'. Among them, there are 279 MYB transcription factors and 203 bHLH transcription factors (Supplementary Table S4).

Based on GO and KEGG enrichment, transcription factors (TFs) coded by DEGs and seven structural genes were subjected to protein–protein interaction analysis to screen crucial TFs control anthocyanin synthesis. The results are

displayed (Supplementary Table S4): bHLH2 (gene-LOC120149108), bHLH4 (gene-LOC120171442), bHLH6 (gene-LOC120209233), bHLH7 (gene-LOC120215242), MYB1 (Hibiscus_syriacus_newGene_28382), MYB3 (gene-LOC120154943), and MYB5 (gene-LOC120214348) would possibly participate in the regulation of the seven structural genes.

qRT–PCR analysis validation of anthocyanin synthesis structural genes

To verify the accuracy of the RNA-Seq results, we designed seven structural genes and seven regulatory genes in flavonoid metabolism and analyzed the relative expression quantities in the five flowering stages through qRT–PCR (Fig. 5). The change trend of relative expression was consistent with that of substance content, which indicated that the result of RNA-Seq was reliable.

Discussion

Petal color transition is attributed to the changes within the accumulation of the foremost anthocyanins

Through the mixture of metabolome and transcriptome, the explanations for the amendment of flower color of the *H. syriacus* 'Qiansiban' from S1 to S5 were explored. A recent research on *H. syriacus* has found that there are a minimum of 40 different anthocyanidin components; cyanidin, delphinidin, and malvidin have been detected [8]. Our analysis results show that anthocyanins are the main component of *H. syriacus* petal color display, which is the same as the previous analysis results (Fig. 1 and Table 1). A total of 5 anthocyanins were detected in petals at five stages. With the gap method, the content of anthocyanidin step by step was minimized, whereas the species remained unchanged. Through the analysis of floral leaf pigment composition and content throughout the flowering of the 'Qiansiban', it was found that the amendment of flower color was closely associated with the pigment composition and content in petals. This study showed that the decrease in anthocyanin content was the most reason for the amendment of flower color from purple to pink to purple throughout the flowering method of *H. syriacus*. For instance, rule YANG et al. [26] studied 2 paeony varieties and found that their petals were modified from red to yellow throughout flowering, and their pigment sorts failed to amend, chiefly thanks to the sharp decrease in anthocyanin content. ZHOU B et al. [2] found in their analysis on *Mirabilis jalapa* L that the redness flowers modified from lightweight inexperienced in the bud stage to purple red fully bloom, which was closely associated with the reduction in chlorophyll content and therefore the increase in anthocyanin content. The higher than analysis results support our conclusion to an explicit extent.

Flavonoe and flavonol are chiefly used as auxiliary pigments in flowers to help present anthocyanins; however, they are lightweight yellow. The petals of 'Qiansiban' contain flavonoe and flavonol substances throughout the flowering process. DENG [6] found that flavonoes and flavonols play a vital role in the formation of yellow lotus (*Nelumbo nucifera* Gaertn.). Additionally, luteolin, apigenin-7-*O*-glucoside, kaempferol-3-*O*-glucoside, and different substances are extremely expressed in *Camellia nitidissima* C. W. Chi [27], florist's chrysanthemum [28] and different plants.

The petal color transition is attributed to changes in the accumulation of the foremost anthocyanins.

Anthocyanin early biogenesis genes chiefly embrace genes settled at the upstream of the anthocyanin synthesis pathway, chiefly together with PAL, CHS, CHI, and different genes, that are liable for cryptography flavonoids, flavonol, and different flavonoid synthesis enzymes. Later biogenesis genes chiefly embrace DFR, ANS, UFGT, and different

downstream anthocyanin biogenesis genes, that are chiefly liable for cryptography anthocyanin synthesis enzymes [29]. The expression quantity of most structural genes within the flowers of 'Qiansiban' reached the most within the S2 amount, and so step by step minimized with the gap method of the flowers. This can be contrary to the analysis of paeony [3] and paeony [13]. The expression quantity of paeony and paeony reached the most within the blooming amount, and therefore, the total anthocyanin content and composition of mallow were step by step reduced throughout the flowering method. This can be equivalent to most of the organic phenomenon, that is, the method of flower color accumulation within the early stage. The FLS factor is the key factor for flavonol synthesis. Additionally, to aid in anthocyanin coloration, flavonol can appear lightweight yellow once it is high in content. Whether the expression of FLS causes a rise in flavonol content has to be additionally verified. The DFR chiefly catalyzes dihydroflavonol to synthesize colorless anthocyanins, whereas the ANS chiefly catalyzes colorless anthocyanins to make colored anthocyanins [30]. However, the high expression of most genes in S2, S3, and different early flowering stages promoted the synthesis of anthocyanins within the late stage. The reduction in organic phenomena within the later 2 stages resulted in a reduction in anthocyanin content, leading to changes in flower color [1]. The analysis of chrysanthemums [31] and different decorative plants has additionally verified this time. It is speculated that the DFR, CHI, and FLS genes play a vital role in the amendment of flower color throughout the flowering of *H. syriacus* 'Qiansiban' (Fig. 6).

The relationship between transcription factors and regulatory genes

The transcription factors MYB and bHLH affect the amendment of flower color by regulating the expression of structural genes within the anthocyanin metabolism pathway. In recent years, studies on liliaceous plant bulbs [32], peach [33], mulberry [34], and different plants in Lanzhou have shown that MYB and bHLH are key transcription factors for plant anthocyanin synthesis. During this study, MYB3 and bHLH2, bHLH4, bHLH6, and bHLH7 showed an important negative or direct correlation with UFGT, CHI, CHS, and different genes, during which bHLH7 additionally showed a truly important direct correlation with the entire anthocyanin content. MYB3 and bHLH2, bHLH4, bHLH6, and bHLH7 were associated with the amendment of *H. syriacus* 'Qiansiban' flower color (Supplementary Table S5).

Conclusion

Through metabolome and transcriptome sequencing and qRT—PCR analysis, the color amendment of *H. syriacus* 'Qiansiban' petals from S1 to S5 was studied. The color of its petals changes from red to pink purple and eventually to purple, which is attributed to the reduction in anthocyanin content. Anthocyanidin embrace delphinidin-3-*O*-glucoside, cyanidin-3-*O*-glucoside, petunidin-3-*O*-glucoside, pelargonidin-3-*O*-glucoside, and malvacin-3-*O*-glucoside. According to the transcriptome sequencing results, the interaction of structural genes (DFR, CHI, and FLS) and regulatory genes (MYB3 and bHLH2, bHLH4, bHLH6, and bHLH7) affected the amendment of *H. syriacus* flower color.

Declarations

Data availability statement

All transcriptomic sequencing data associated with this study have been submitted to the NCBI SRA under the accession number PRJNA995230.

Supplementary Material

See Attachment

Author contributions

Zhezhe LI prepared samples for analysis, determined and analyzed the data, interpreted the results and wrote the original draft paper. Dan LIU determined and analyzed the data, interpreted the results Meng SUN , Dongsheng WANG and Yu WU measured supplementary experimental data. Yidan ZHANG collected samples and assisted. Dongsheng WANG and Beibei CHENG designed the study, analyzed the data, interpreted the results and revised the manuscript. Guojun ZHANG made revisions to the first draft of the article.

Acknowledgments

We thank the transcriptome sequencing at Biomarker Technologies Co., Ltd (Beijing, China).

Conflicts of interest

The authors hereby declare no conflicts of interest.

Funding

The work was supported financially by the Survey of Herbal Plant Germplasm Resources in Shandong Province (LCYZ [2021] No. 1); Project of Hebei University Horticultural Crop Breeding Application Technology Research and Development Center (YF201404); Hebei Provincial Professional Degree Graduate Training Practice Base (Tangshan Botanical Garden, 202018); and Germplasm Resources Bank of National Forestry and Grassland Administration (2005DKA210003).

Ethics approval and consent to participate

Our research did not involve any human or animal subjects, material, or data. We declare that the plant material in the experiment was collected and studied in accordance with relevant institutional, national, and international guidelines and legislation.

Consent for publication

Not applicable.

References

1. GUO L P, WANG Y J,et al. Transcriptome and chemical analysis reveal putative genes involved in flower color change in Paeonia ‘Coral Sunset’. Plant Physiology and Biochemistry. 2019; (138):130-139.
2. ZHOU B, YAN X H, LEI Y H, et al. Variation of flower color and pigment contents of Mirabilis jalapa during flowering. Bulletin of Botanical Research. 2022; 42(3): 475-482.
3. Zhao D, Tao J, Han C, et al. Flower color diversity revealed by differential expression of flavonoid biosynthesis-related genes and flavonoid accumulation in herbaceous peony (Paeonia lactiflora Pall.). Molecular biology reports. 2012; 39(12):11263-11275.
4. ZHENG X D, PAN X X, MENG X M, et al. Research progress in determination of carotenoids in Lycium chinense by HPLC. China Fruit & Vegetable. 2013; (10): 27-30.

5. TANAKA Y, SASAKI N, OHMIYA A. Biosynthesis of plant pigments: anthocyanins, betalains and carotenoids. The Plant Journal. 2008; 54(4): 733-749.
6. Deng J, Chen S, Yin X J, et al. Systematic qualitative and quantitative assessment of anthocyanins, flavones and flavonols in the petals of 108 lotus (Nelumbo nucifera) cultivars-ScienceDirect. Food Chem. 2013; 139(1—4): 307–312.
7. Li X, Duan JJ, Luo XN, et al. Formation mechanism of different tree peony flower colors by anatomy and biochemistry. J Northeast For Univ. 2019; 43 (3):38–43.
8. ZHANG P, LI Y, CHONG S L, et al. Identification and quantitative analysis of anthocyanin composition and stability from different strains of Hibiscus syriacus L. flowers. Industrial Crops Products. 2022; (177):114457.
9. CHEN J L, HOU R M, ZHU J J, et al. RNA sequence analysis of petals of two cultivars of Hibiscus syriacus with different flower colors. Molecular Plant Breeding. 2022; 20(8): 2507-2516.
10. HE Y F, ZHANG C Y, LIU Q L. Characterization of flower coloration in petals of Rhododendron simsii. Journal of Agricultural Science and Technology. 2021; 23(2): 50-56.
11. GAO S, LI T L. Relationship between the compositon of anthocyanins and flower color variation in lisianthus(Eustoma grandiflorum). Journal of Shenyang Agricultural University. 2020; 51(4): 410-416.
12. CUI H L, HE X, ZHANG Q. Dynamic changes of anthocyanin and flavonoid composition in petals of different peony varieties during account opening. Scientia Agricultura Sinica. 2021; 54(13): 2858-2869.
13. YANG C. Analysis of petal pigment composition and related gene expression during flower color change of 'Fengdan' Peony. Yangling: Northwest University of agriculture and forestry science and technology. 2020.
14. CHEN H. Analysis of anthocyanin components and antioxidant capacity of Hibiscus syriacus with different flower color. Qinhuangdao: Hebei Normal University of Science and Technology. 2021.
15. WANG X T, LI X G, LI D L, et al. Identification and analysis of nonanthocyanin phenolics in various raspberry (Rubus spp.) cultivars. Northern Horticulture. 2021; (11): 36-43.
16. Buchfink B, Xie C, Huson DH. "Fast and sensitive protein alignment using DIAMOND", Nature Methods. 2015; (12): 59-60.
17. Deng YY, Li JQ, Wu SF, Zhu YP, et al. Integrated nr Database in Protein Annotation System and Its Localization. Computer Engineering. 2006; 32(5):71-74.
18. Apweiler R, Bairoch A, Wu CH, et al. UniProt: the universal protein knowledgebase. Nucleic acids research. 2004; 32: D115-D119.
19. Tatusov RL, Galperin MY, Natale D A. The COG database: a tool for genome scale analysis of protein functions and evolution. Nucleic Acids Research. 2000: 28(1):33-36.
20. Koonin EV, Fedorova ND, Jackson JD, et al. A comprehensive evolutionary classification of proteins encoded in complete eukaryotic genomes. Genome biology. 2004; 5(2): R7.
21. Kanehisa M, Goto S, Kawashima S, Okuno Y, et al. The KEGG resource for deciphering the genome. Nucleic Acids Research. 2004; 32:D277-D280.
22. Jones P, Binns D, Chang H Y, et al. InterProScan 5: genome-scale protein function classification[J]. Bioinformatics. 2014; 30(9): 1236-1240.
23. Ashburner M, Ball C A, Blake J A, et al. Gene ontology: tool for the unification of biology. Nature genetics2000; 25(1): 25-29.
24. Eddy S R. Profile hidden Markov models. Bioinformatics.1998; 14(9): 755-763.

25. Finn RD, Bateman A, Clements J, et al. Pfam: the protein families database. Nucleic acids research. gkt1223. 2013.
26. YANG Q, YUAN T, SUN X B. Preliminary studies on the changes of flower color curing the flowering period in two tree peony cultivars. Acta Horticulturae Sinica. 2015; 42(5): 930-938.
27. Li X L, Wang J T, Sun Z Y, et al. The relationship between flavonoid components and flower color of Camellia japonica, Camellia alba, and their three hybrid varieties. Journal of Horticulture. 2019; 46 (6): 1145-1154.
28. Xie Z F, Zhang Q Q, Zhu L J, Han G. Research progress on chemical components and pharmacological activities of chrysanthemum. Journal of Henan University (Medical Edition). 2015; 34 (4): 290-300.
29. Luo T J. Research progress on genes related to plant Anthocyanidin metabolism pathway. Southern Agriculture. 2022; 16 (16): 202-206.
30. DAI S L, HONG Y. Molecular breeding for flower color improvement of ornamental plants based on the mechanism of Anthocyanidin glycoside synthesis and color rendering. China Agricultural science. 2016; 49 (3): 529-542.
31. HAN K T. Effects of the introduction of key structural genes for anthocyanidin glycoside synthesis on chrysanthemum flower color. Beijing: Beijing Forestry University. 2010.
32. FAN W G, LI B Y, TIAN H, et al. Screening and analysis of MYB and bHLH transcription factors related to Anthocyanidin synthesis in lily bulbs of Lanzhou [J/OL]. Food and fermentation industry: 1-12 [2023-08-03]. DOI: 10.13995/j.cnki.11-1802/ts.033270 https://kns.cnki.net/kns8/defaultresult/index.
33. HUA Y, LV X Y, ZHANG Y, et al. Research progress of peach MYB transcription factor regulating Anthocyanidin synthesis. Modern Agricultural Science and Technology. 2022; (21): 75-79.
34. FAN Y T. Research on the Regulation and Mechanism of Mulberry MYB61 Gene on Anthocyanidin and Lignin Synthesis. Tai'an: Shandong Agricultural University. 2022.

Figures

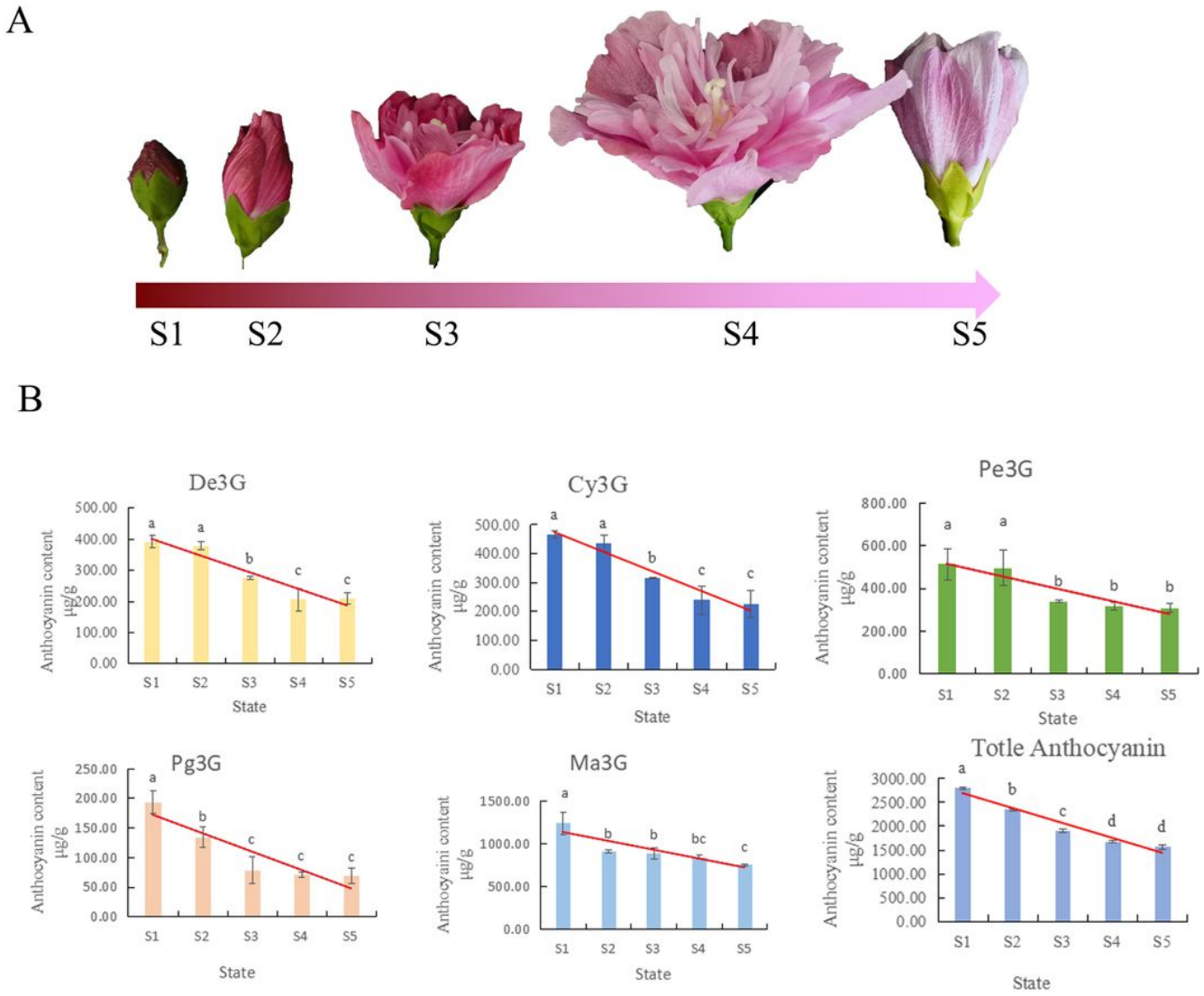

Figure 1

Content of anthocyanins in the 'Qiansiban' petals at different stages. (A)

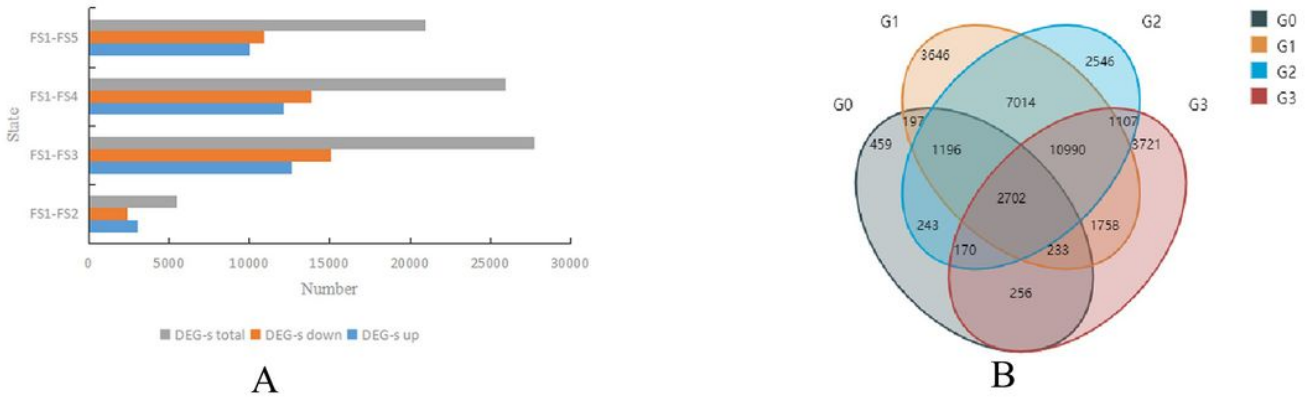

Figure 2

Overview of the *H. syriacus* petal transcriptome. (A) Statistics of differential expressionbetween petals harvested atdifferent developmental stages. (B) Venn diagram representing a common and specific number of DEGs between the three comparisons. where G0:S1 VS S2; G1:S1 VS S3; G2:S1 VS S4; G3:S1 VS F5, and S1-S5 represent flower development stages.

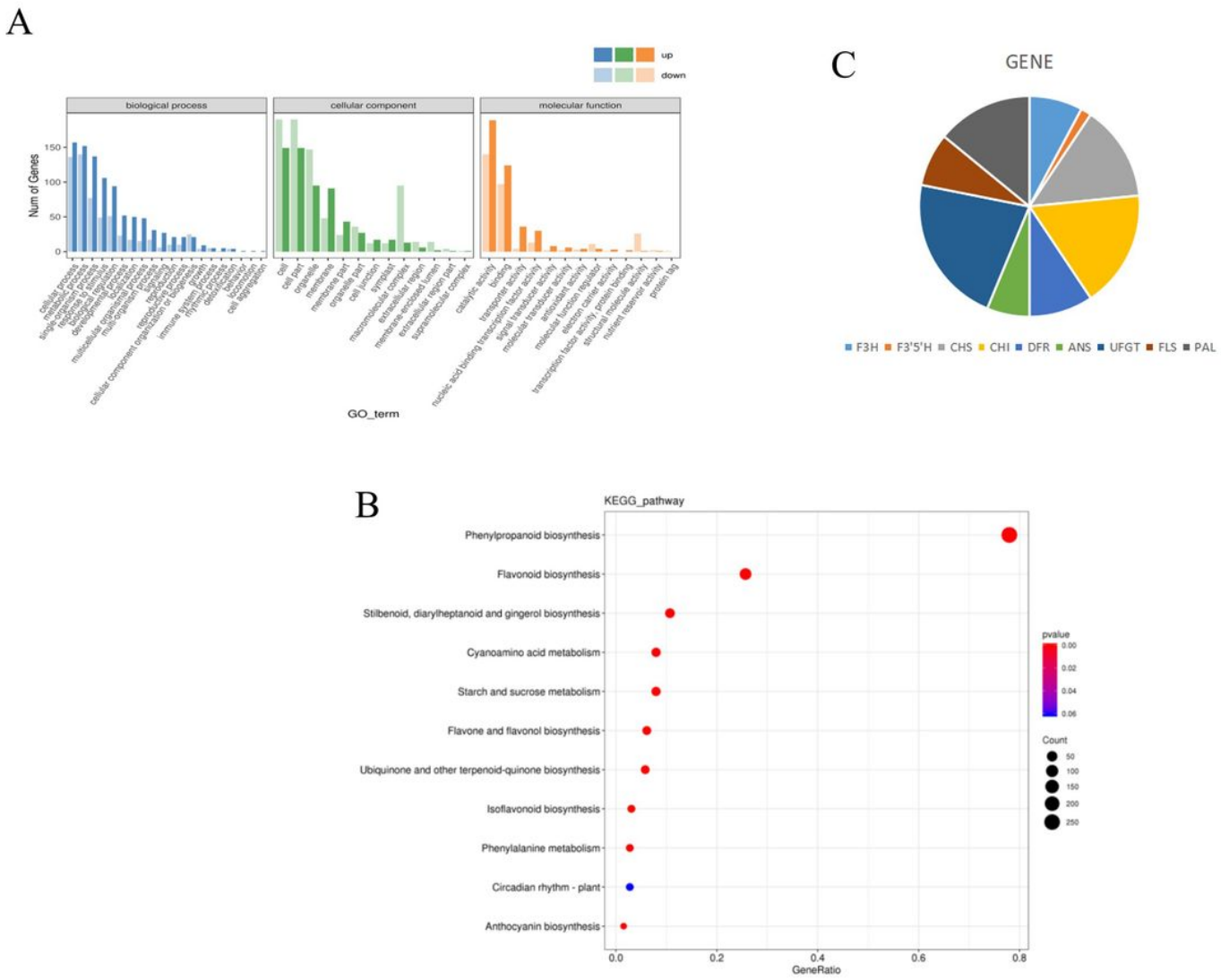

Figure 3

Differential gene analysis (A): Differential expression gene GO annotation classification statistical chart. (B): Metabolic pathway map of KEGG differential genes in *H. syriacus* 'Qiansiban'. (C): Number of differentially expressed genes.

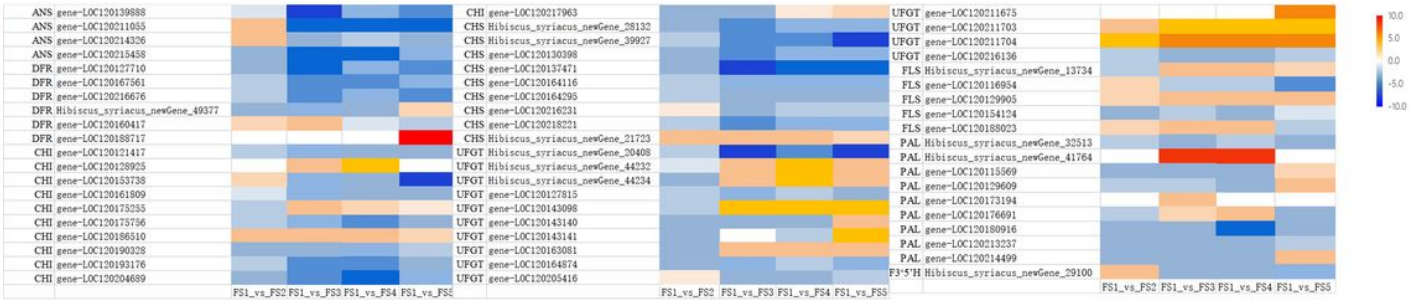

Figure 4

Heatmaps (log2(fold change)) of the anthocyanin biosynthesis genes. S1 (Splitting stage), S2 (Early stage), S3 (Initial opening period), S4 (Blooming period), and S5 (Final flowering stage) represent flower development stages.

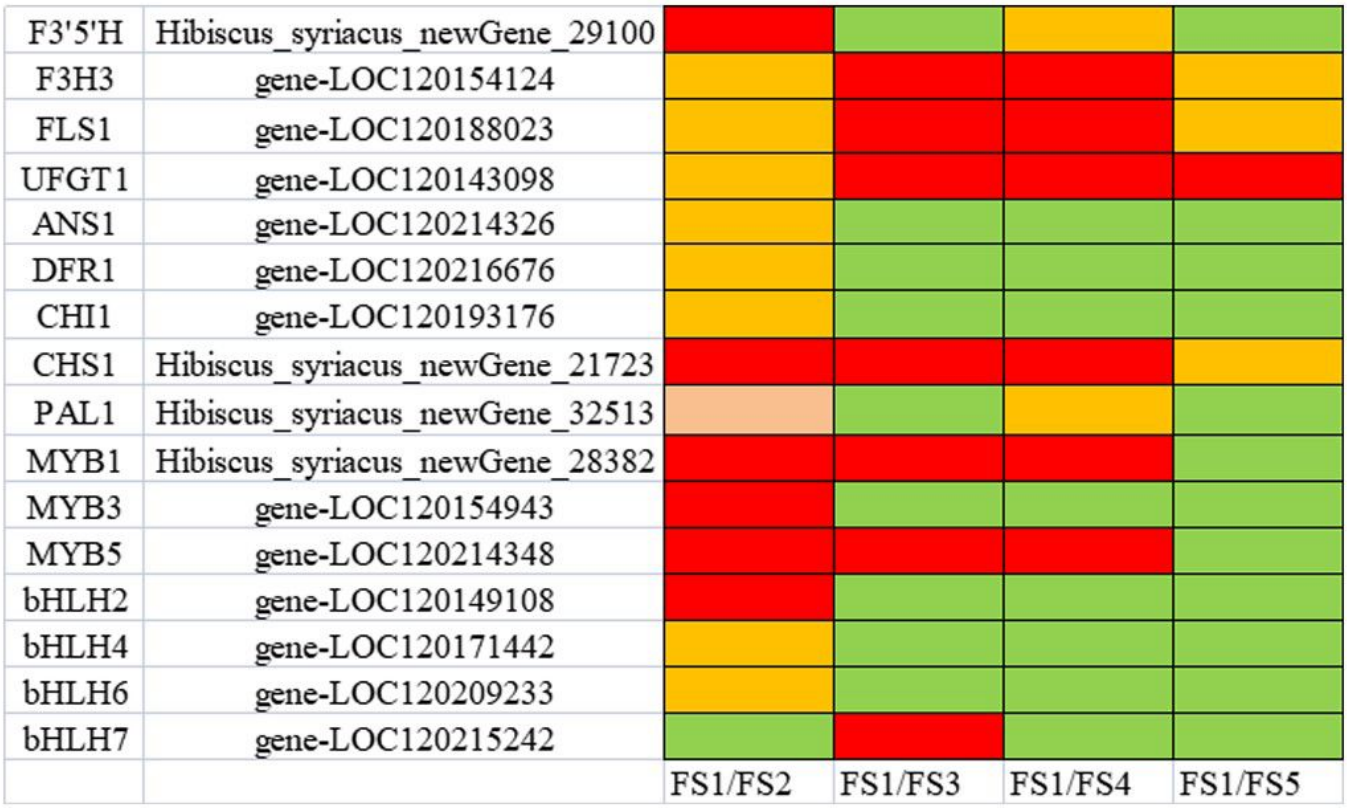

Figure 5

qRT—PCR expression of anthocyanin-related genes. The heatmaps show the change in expression from one stage to the other. The color of the boxes represents lower (green) to higher (red) relative change values.

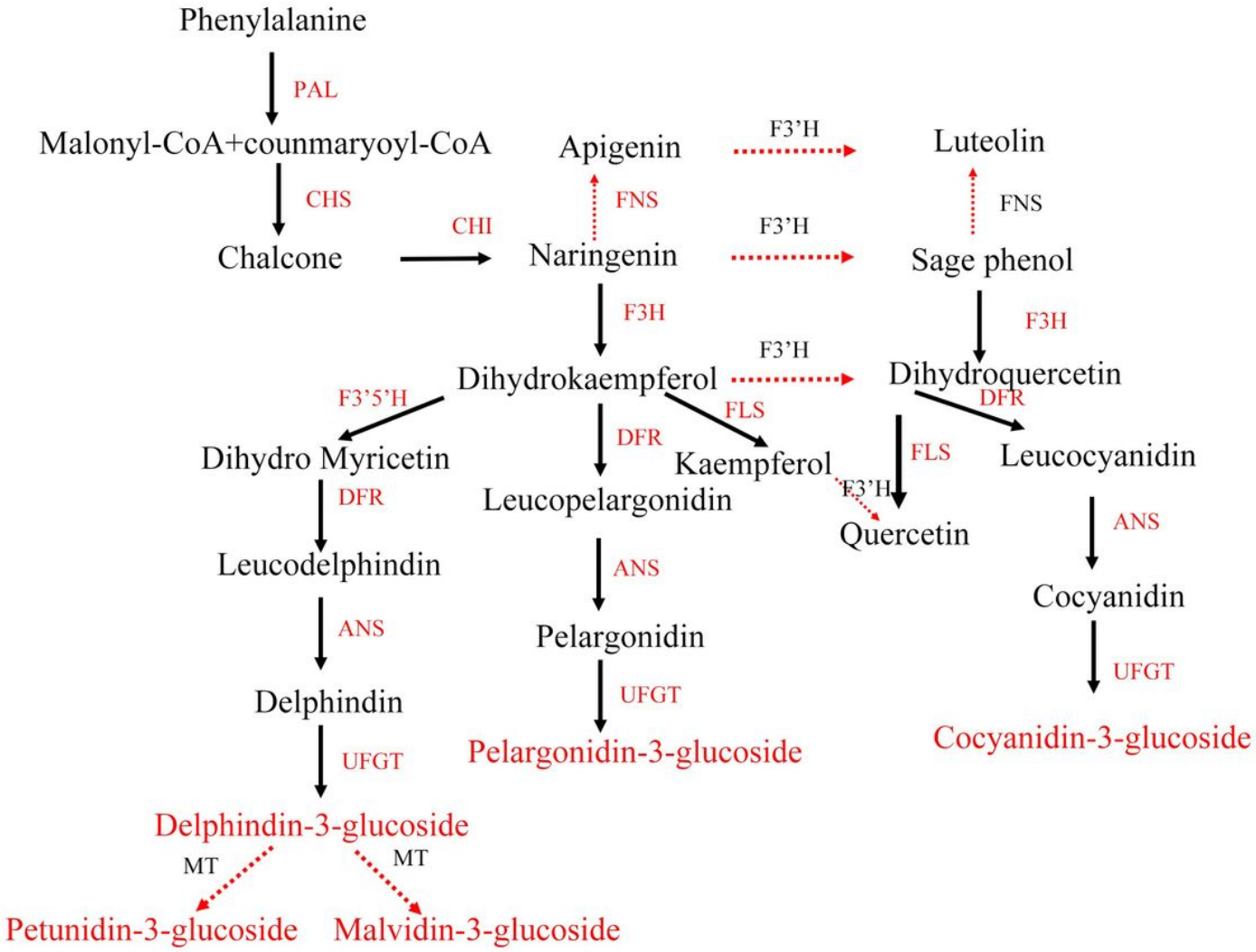

Figure 6

Differential regulation of anthocyanin biosynthesis in *H. syriacus* petals. The genes and metabolites that were differentially expressed and accumulated, respectively, are given in red text. The dotted arrows/lines indicate that the genes are not found or not known. According to the transcriptome and metabolome data, refer to the KEGG metabolic pathway and draw a flow chart. The gene name abbreviations correspond to the full names given in Supplementary Table S6.

Supplementary Files

This is a list of supplementary files associated with this preprint. Click to download.

- SupplementaryFigureS1.png
- SupplementaryTable16.xlsx